Supporting Information for

$NaFeF_3$ Nanoplates as Low-Cost Sodium and Lithium Cathode Materials for Stationary Energy Storage

Kostiantyn V. Kravchyk,[†,‡] *Tanja Zünd,*[†,‡] *Michael Wörle,*[†] *Maksym V. Kovalenko,*[*,†,‡] *and Maryna I. Bodnarchuk* [*,‡]

[†] Laboratory of Inorganic Chemistry, Department of Chemistry and Applied Biosciences, ETH Zürich, Vladimir-Prelog-Weg 1, CH-8093 Zürich, Switzerland

[‡] Laboratory for Thin Films and Photovoltaics, Empa – Swiss Federal Laboratories for Materials Science and Technology, Überlandstrasse 129, CH-8600 Dübendorf, Switzerland

Corresponding Authors:

*E-mails: maryna.bodnarchuk@empa.ch and mvkovalenko@ethz.ch

Synthesis

Synthesis of sodium hexafluoroacetylacetonate - Na(hfac). In a typical synthesis, 4 g (0.1 mol) NaOH (Merk) was dissolved in 150 mL distilled water at room temperature under ambient conditions. 15.5 mL of hexafluoroacetylacetone (0.11 mol, STREM) were added to the NaOH/water solution. Reaction mixture was stirred for 1.5 hr with further evaporation of water by rotary evaporator. White powder of Na(hfac) was placed under vacuum at 50 °C for 30 min for complete drying. Na(hfac) had been stored in a glovebox.

Synthesis of $NaFe(hfac)_3$. Synthesis of $NaFe(hfac)_3$ was performed as describe in Ref.[1] In a typical synthesis, Na(hfac) (4.36 g, 18.9 mmol) and $FeCl_2$ (anhydrous, 0.8 g, 6.3 mmol, ABCR) were dissolved in 120 mL anhydrous acetone under argon atmosphere. The reaction mixture was stirred at room temperature for 2 hr. The solution was filtered into another flask under argon and the solvent was evaporated by rotary evaporator. Obtained product was further dried under vacuum at room temperature. Final powder had purple color and had been stored in glovebox.

Synthesis of $NaFeF_3$ nanoplates (NPLs). In a typical synthesis oleic acid (0.5 mL, Sigma-Aldrich, 90%), oleylamine (0.5 mL, STREM, 95%) and benzyl ether (5 mL, Sigma-Aldrich) were loaded into a 25-mL flask and dried at 90 °C for 1 hr. Then, $NaFe(hfac)_3$ (0.5 mmol, 0.35 g) were added to the flask under argon forming homogenous purple solution. The reaction mixture was heated up to 260 °C and kept at this temperature for 1 hr. The color of the solution has changed from purple to brown, indicating decomposition of the precursor and formation of NPLs. $NaFeF_3$ NPLs were washed 2 times by chloroform/ethanol mixture and separated by centrifugation. After the second washing step, NPLs were re-dispersed in chloroform (2-3 mL) and stored under ambient condition. Equal results were obtained using octadecene as a solvent instead of benzyl ether.

N_2H_2-treatment of $NaFeF_3$ NPLs. Prior to electrode preparation, organic ligands from the surface of $NaFeF_3$ NPLs were removed by stirring NPLs in a 0.1 M solution of hydrazine in acetonitrile for 10-15 min at room temperature under argon atmosphere, followed by centrifuging. Such procedure was repeated 4 times.

Electrochemical measurements

Battery components. Carbon black (Super C65, TIMCAL), pvdf (Poly(vinylidene flouride), MW~534000, Aldrich), carboxymethyl cellulose (CMC, Grade: 2200, Lot No. B1118282, Daicel Fine Chem Ltd.), NMP (99%, Sigma Aldrich), $NaClO_4$ (98%, Alfa Aesar, additionally dried), propylene carbonate (BASF, battery grade), 4-fluoro-1,3-dioxolan-2-one (FEC, Hisunny Chemical, battery grade), 1 M solution of $LiPF_6$ in ethylene carbonate/dimethyl carbonate (EC/DMC, Novolyte, Celgard separator (Celgard 2400, 25μm microporous monolayer polypropylene membrane, Celgard Inc. USA), glass microfiber separator (GF/D, Cat No.1823-257, Whatman), Al foil (MTI Corporation), Na foil (Sigma-Aldrich), Li foil (MTI Corp.), Sb (99.5%, Alfa Aesar), Coin-type cells (Hohsen Corp., Japan).

Assembly and testing of Na- and Li-ion cells. After ligand removal, $NaFeF_3$ NPLs (50 wt. %) were mixed with carbon black (25 wt. %) and graphene oxide (10 wt. %), following ball milling at 500 rpm for 3 hr and heat-treatment at T=300°C for 1hr under nitrogen atmosphere. Then, obtained mixture was mixed with pvdf binder (10 wt. %) in NMP and ball milled for 1h. Obtained slurry was painted onto Al foil which was then dried for 12 hr at 80°C under vacuum. Coin-type cells were assembled in an argon-filled glove box (O_2 < 1 ppm, H_2O < 1 ppm) using one layer separator (glass fiber) for NIBs and two layers of separators (Celgard and glass fiber) for LIBs. Elemental sodium or lithium served as both reference and counter electrodes. As electrolyte 1 M $NaClO_4$ in PC was used for Na-ion batteries and 1 M $LiPF_6$ in EC:DMC (1:1 by wt.) for LIBs batteries. To improve cycling stability 3 wt. % of FEC were added to both electrolytes.

Electrochemical measurements were performed on a MPG2 multi-channel workstation (Bio-Logic) using current density of 0.2 A g^{-1} (0.1 mA cm^{-2}) between 1.5-4 V and 2-4.2 V for Na ion and Li ion cells, accordingly. Constant current constant voltage (CCCV) mode was applied for charge step. The constant voltage (4 V or 4.2 V) was kept until measured current was equal to 1/10 of the initial current value. The obtained capacities were normalized to the mass of $NaFeF_3$ NPLs.

Characterization. TEM and STEM studies were performed using JEOL JEM-2200FS microscope operated at 200 kV, and FEI Talos F200X operated at 200kV and equipped with Super-X EDS system (4 detector configuration). EDS-STEM elemental analyses were complemented by the elemental content studies by EELS performed on a Hitachi HD-2700 microscope operated at 200 kV. EELS spectra was acquired in the STEM operation mode and analyzed using Digital Micrograph (Gatan). Powder X-ray diffraction pattern was collected with STOE STADIP powder diffractometer.

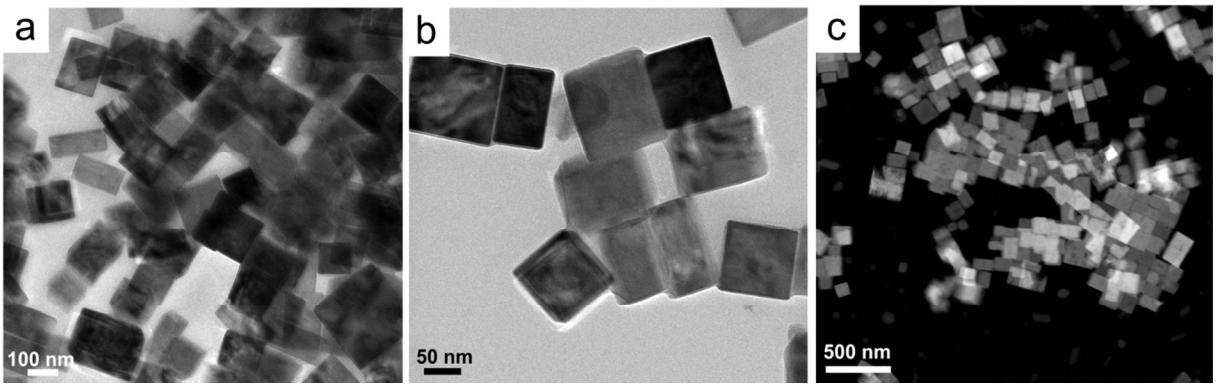

Figure S1. (a, b) TEM and (c) STEM images of $NaFeF_3$ NPLs.

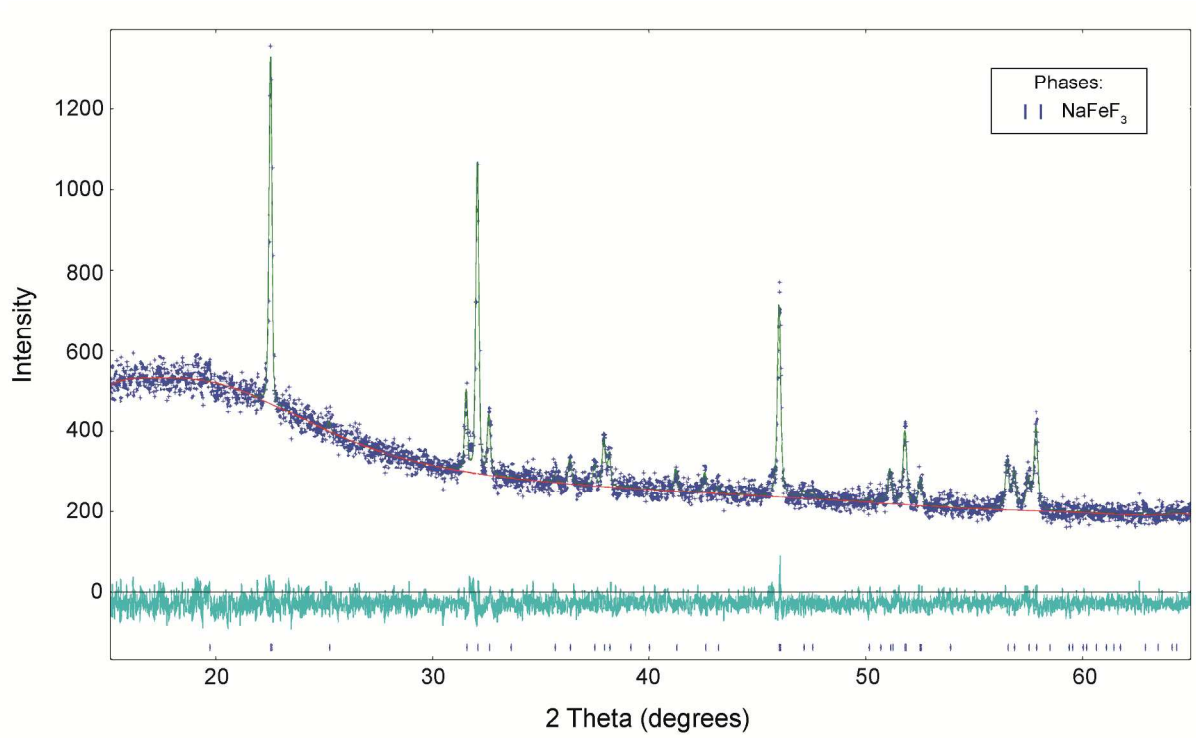

Figure S2. A comparison of the experimental (blue crosses) and calculated (green) powder diffraction pattern of $NaFeF_3$ together with the difference (light blue) and the reflection positions (blue markers), as obtained from the Rietveld refinement with GSAS-II.[2] The refinement was performed using the structural data from ICSD 6898.[3] The orthorhombic lattice parameters refined to a = 5.6651(4) Å, b = 7.8869(6) Å and c = 5.4879(4) Å, which are slightly larger than the ones given in Ref.[3] as a = 5.6575(9) Å, b = 7.8754(13) Å and c = 5.4833(11) Å. Considering that the standard uncertainties of Rietveld refinements neglect systematic errors and are therefore largely underestimated, the deviations between the observed and expected values are not regarded as significant. The figure of merits are R(F) = 16.64%, $R(F^2)$ = 18.78% on 48 reflections, wRp = 5.25%, χ^2 = 4370.53, GOF = 0.94. The sample is phase pure and shows no reflection broadening due to crystallite size with respect to the micrometer sized standard sample (Si, NBS 640c), however a significant contribution of isotropic microstrain of $\Delta d / d * 10^6 = 4876(79)$.

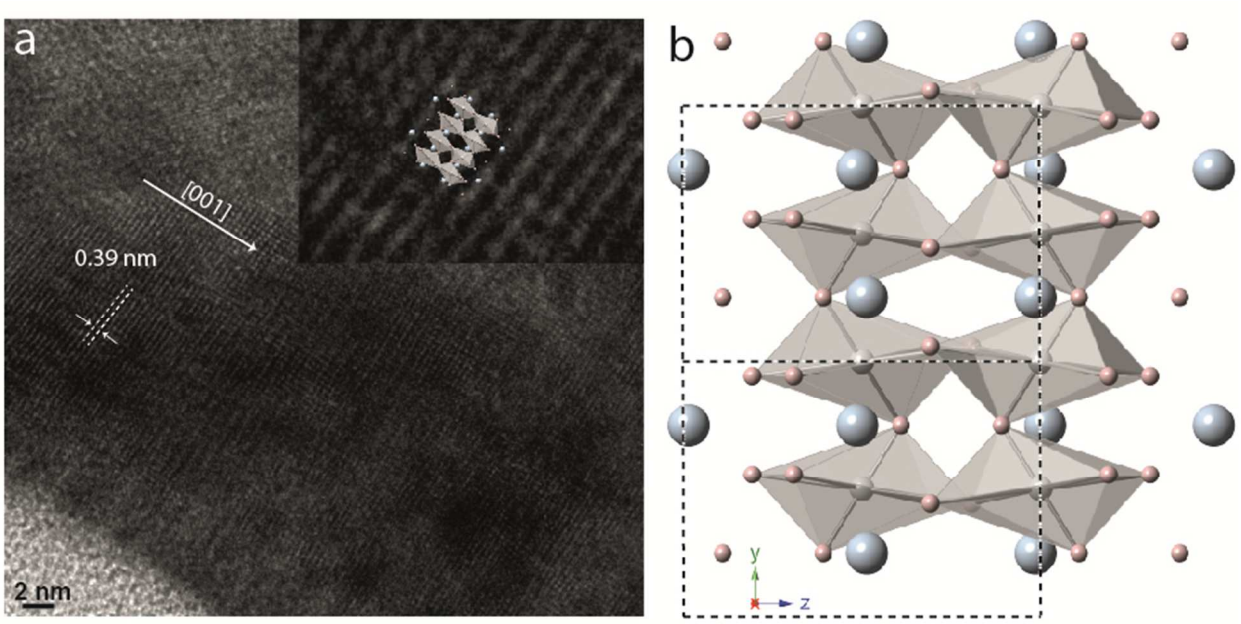

Figure S3. (a) HRTEM image and (b) orthorhombic structures of $NaFeF_3$ NPLs with the top facet being (100) plane.

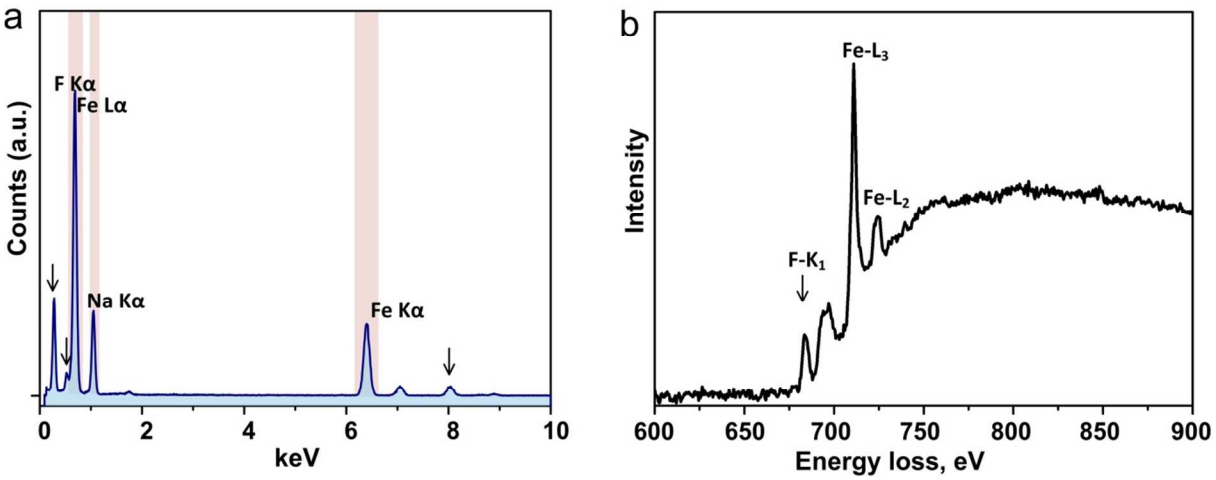

Figure S4. (a) EDX-spectrum of $NaFeF_3$ NPLs (arrows on the graph indicate Cu from the metallic support grid, C and O picks which appeared due to grid or partial surface oxidation of NPLs). (b) Characteristic EELS spectra of $NaFeF_3$ NPLs.

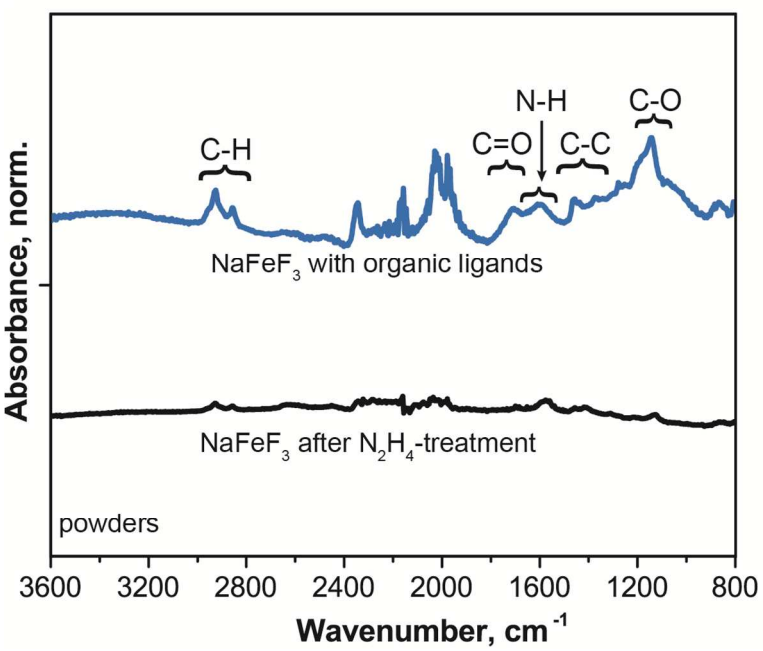

Figure S5. FTIR spectra of $NaFeF_3$ NPLs before (after the synthesis) and after ligand removal. The absence of C-H, C=O, N-H, CC and C-O bonds after ligand removal indicated that all organic ligands were removed by hydrazine treatment.

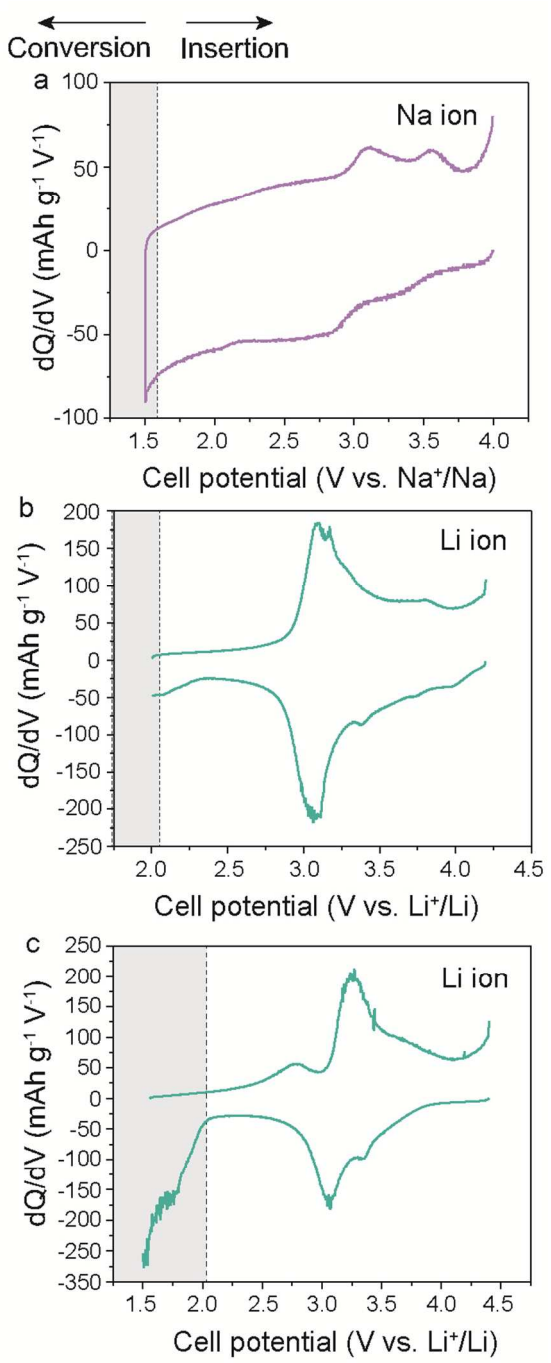

Figure S6. Typical differential capacity plots of $NaFeF_3$ NPLs obtained from galvanostatic discharge/charge curves at a current density of 0.2 A g^{-1}. $NaFeF_3$ NPLs were cycled with sodium and lithium electrolytes in a half-cell configuration using metallic sodium and lithium as the counter and reference electrodes, respectively. Conversion and insertion regions are shown by gray and white colors. As follows from differential capacity plots of $NaFeF_3$ NPLs (a, b), conversion reaction starts at about 1.5 V *vs.* Na^+/Na and 2V *vs.* Li^+/Li indicating that 1.5-4 V and 2-4.2 V voltage intervals correspond primarily to the insertion region. Further decreasing of voltage interval (c) causes sharp increasing of dQ/dV negative intensity indicating the start of conversion reaction.

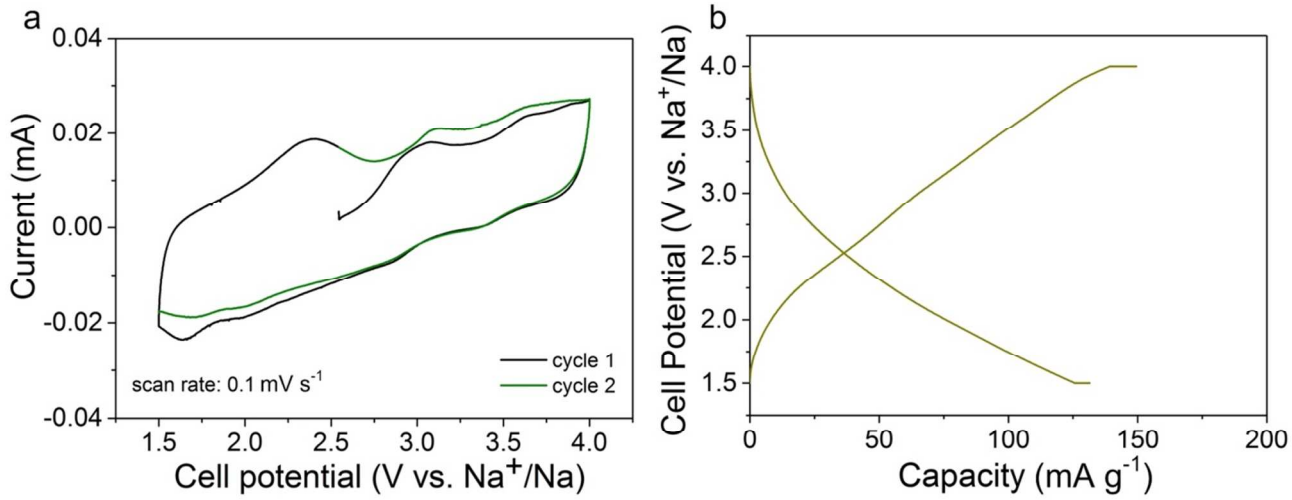

Figure S7. (a) Cyclic voltammetry curves of cathode composed of $NaFeF_3$ NPLs measured in Na electrolyte at scan rate of 0.1 mV s^{-1}. (b) Galvanostatic charge-discharge curves of cathode composed of $NaFeF_3$ NPLs during 10^{th} cycle measured in Na electrolyte at current density of 20 mA g^{-1}.

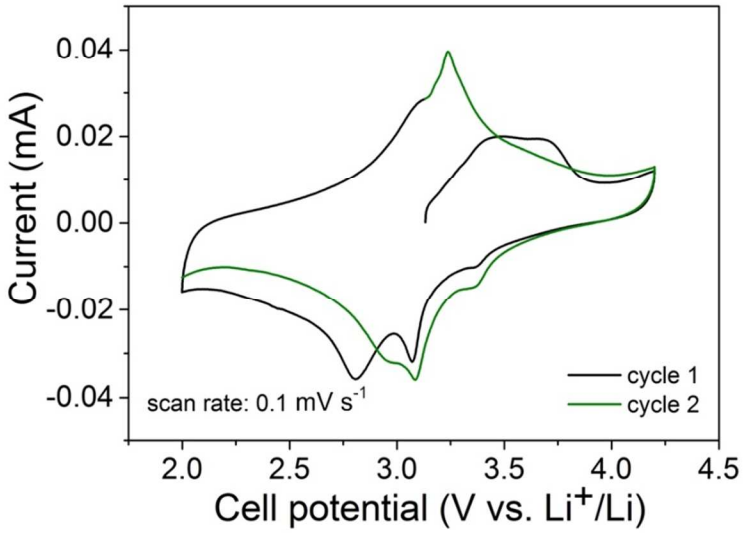

Figure S8. Cyclic voltammetry curves of cathode composed of $NaFeF_3$ NPLs measured in Li electrolyte at scan rate of 0.1 mV s^{-1}.

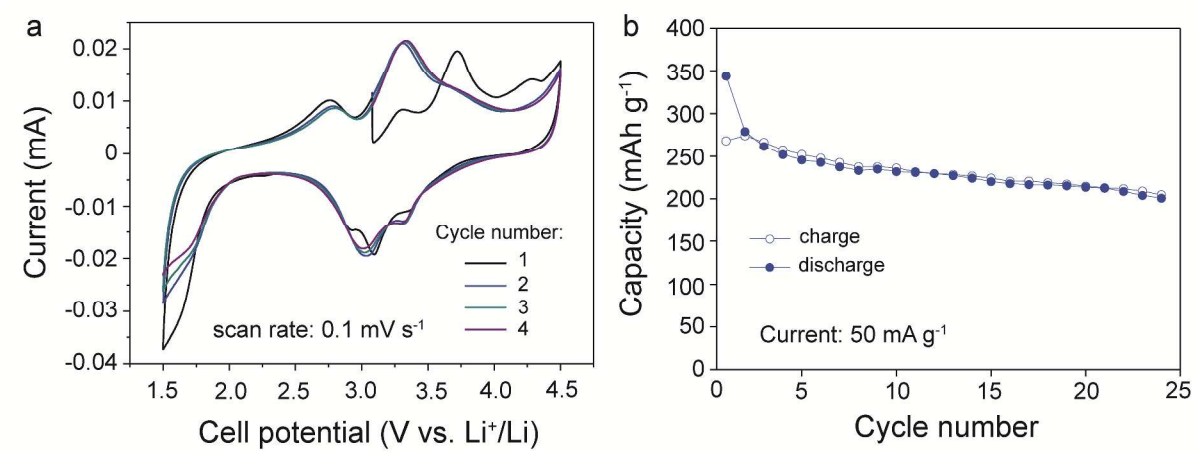

Figure 9. Cyclic voltammetry (a) and cyclic stability (b) measurements of $NaFeF_3$ NPLs cycled with lithium electrolytes using 1.5-4.2 V voltage interval which includes both conversion (1.5-2.0 V *vs.* Li^+/Li) and insertion (2.0-4.2 V *vs.* Li^+/Li) regions, respectively.

Table S1. Reflection list of $NaFeF_3$ NPLs.

h,k,l	2-theta	F_obs	F_calc	phase	mult	sig	gam	FWHM	Prfo
3,2,2	19.722	264.169	15.492	0	4	0.04107	0.03573	0.11672	1
0,2,0	22.559	6292.061	4165.092	0	2	0.04095	0.04333	0.12113	1
1,0,1	22.569	6696.152	4444.96	-180	4	0.04095	0.04336	0.12115	1
1,1,1	25.269	368.731	124.026	180	8	0.04084	0.05066	0.12555	1
2,0,0	31.59	7988.576	6501.981	0	2	0.04059	0.06803	0.1366	1
1,2,1	32.11	7681.154	6616.754	180	8	0.04057	0.06948	0.13755	1
0,0,2	32.637	6362.85	5158.859	0	2	0.04055	0.07096	0.13853	1
2,1,0	33.62	109.166	30.28	0	4	0.04051	0.07371	0.14037	1
2,0,1	35.67	816.004	380.222	180	4	0.04043	0.07951	0.14428	1
1,0,2	36.38	1984.926	1495.32	-180	4	0.04041	0.08153	0.14566	1
2,1,1	37.505	828.386	634.687	180	8	0.04037	0.08474	0.14788	1
0,3,1	37.947	3760.875	3075.347	0	4	0.04035	0.08601	0.14876	1
1,1,2	38.185	1213.84	1052.635	0	8	0.04034	0.0867	0.14924	1
2,2,0	39.153	472.465	162.974	-180	4	0.04031	0.08949	0.15119	1
0,2,2	40.027	527.475	159.226	0	4	0.04028	0.09203	0.15298	1
1,3,1	41.272	1238.69	853.387	0	8	0.04024	0.09567	0.15556	1
2,2,1	42.605	1176.305	852.558	-180	8	0.04019	0.09959	0.15837	1
1,2,2	43.218	583.824	315.759	-180	8	0.04017	0.10141	0.15969	1
0,4,0	46.021	17001.645	14293.575	0	2	0.04009	0.1098	0.16582	1
2,0,2	46.043	15710.338	13215.092	0	4	0.04009	0.10987	0.16587	1
2,3,0	47.154	1085.71	820.184	0	4	0.04005	0.11324	0.16837	1
2,1,2	47.543	607.243	450.276	180	8	0.04004	0.11443	0.16926	1
2,3,1	50.163	488.383	312.674	-180	8	0.03996	0.12251	0.17534	1
1,3,2	50.704	421.239	232.079	-180	8	0.03995	0.12421	0.17662	1
3,0,1	51.14	5220.352	4670.208	-180	4	0.03994	0.12557	0.17766	1
0,1,3	51.252	358.774	296.876	180	4	0.03993	0.12592	0.17793	1
1,4,1	51.831	2725.103	2439.245	-180	8	0.03992	0.12775	0.17933	1
2,2,2	51.846	3310.038	2966.903	0	8	0.03992	0.1278	0.17936	1
3,1,1	52.531	1424.954	1221.311	-180	8	0.0399	0.12996	0.18103	1
1,0,3	52.555	1770.218	1508.56	-180	4	0.0399	0.13004	0.18109	1
1,1,3	53.92	838.555	279.414	-180	8	0.03986	0.1344	0.18446	1
3,2,1	56.558	5544.816	4402.325	-180	8	0.0398	0.14298	0.19118	1
2,4,0	56.877	7786.497	6991.588	0	4	0.03979	0.14403	0.19201	1
0,4,2	57.539	7400.685	5907.315	0	4	0.03977	0.14622	0.19374	1

1,2,3	57.882	9021.416	8107.064	180	8	0.03976	0.14736	0.19465	1
2,3,2	58.509	2.176	1.438	180	8	0.03975	0.14945	0.19631	1
3,0,2	59.391	81.758	17.869	0	4	0.03973	0.15242	0.19868	1
2,4,1	59.534	59.741	14.931	0	8	0.03973	0.1529	0.19907	1
1,4,2	60.017	106.896	39.191	180	8	0.03972	0.15454	0.20039	1
2,0,3	60.196	1085.547	414.183	0	4	0.03971	0.15514	0.20088	1
3,1,2	60.653	171.755	38.942	0	8	0.0397	0.1567	0.20213	1
0,5,1	61.104	1455.21	479.982	0	4	0.0397	0.15825	0.20338	1
2,1,3	61.448	83.073	12.559	180	8	0.03969	0.15943	0.20434	1
0,3,3	61.755	252.119	20.592	180	4	0.03968	0.16049	0.2052	1
3,3,1	62.891	1527.422	449.295	0	8	0.03966	0.16444	0.20842	1
1,5,1	63.497	0.335	0.043	0	8	0.03965	0.16656	0.21016	1
1,3,3	64.135	728.202	329.616	-180	8	0.03964	0.16881	0.21201	1
3,2,2	64.351	695.603	282.032	0	8	0.03963	0.16958	0.21264	1

Table S2. Comparison of the electrochemical performance of $NaFeF_3$ NPLs (present work) with other reported systems comprising alkali metal fluorides or metal fluorides as cathode materials for lithium and sodium ion batteries.

Cathode material	Current density (mAh g^{-1} or mAh cm^{-2})	Initial capacity ($mAhg^{-1}$)	Retained capacity ($mAhg^{-1}$)	Cycle number	Potential range (V vs. Li^+/Li or Na^+/Na)	System
$NaFeF_3$ NPLs (present work)	200 mAh g^{-1}	153	77	200	1.5-4.0	Na-ion
$NaFeF_3$ NPLs (present work)	200 mAh g^{-1}	183	95	200	2.0-4.5	Li-ion
FeF_3[4]	0.2 mAh cm^{-2}	140	80	2	2.0-4.5	Li-ion
TiF_3[4]	0.2 mAh cm^{-2}	180	80	2	2.0-4.5	Li-ion
FeF_3:C nanocomposite[5]	7.58 mAh g^{-1}	700	600	12	1.5-4.5	Li-ion T=70°C
$NaFeF_3$[6]	0.076 mAh cm^{-2}	197	175	2	1.5-4.5	Na-ion
$NaFeF_3$[7]	1.97 mAh g^{-1}	170-181	-	1	1.5-4.5	Na-ion
$NaFeF_3$[8]	0.2 mAh cm^{-2}	130	90	19	1.5-4.0	Na-ion
$NaMnF_3$[8]	0.2 mAh cm^{-2}	40	32	15	1.5-4.0	Na-ion
$NaNiF_3$[8]	0.2 mAh cm^{-2}	37	24	15	1.5-4.0	Na-ion
Na_3FeF_6[9]	50 mAh g^{-1}	428	296.7	60	1.0-4.5	Li-ion
FeF_3-C composite[10]	0.2 mAh cm^{-2}	200	160	40	2.0-4.5	Li-ion
FeF_3-C composite[10]	0.2 mAh cm^{-2}	145	90	10	1.5-4.0	Na-ion
$NaFeF_3$[11]	7.5 mAh g^{-1}	225	250	10	1.5-4.5	Na-ion
Nano flake/micro-flower FeF_3[12]	237 mAh g^{-1}	187.1	172.3	50	2.0-4.5	Li-ion
FeF_3 NPs[13]	23.7-237 mAh g^{-1}	270	150	55	1.5-4.5	Li-ion
Nanocrystalline FeF_3[14]	100 mAh g^{-1}	220	150	100	2.0-4.2	Li-ion
FeF_3 nanoflowers on CNT[15]	20 mAh g^{-1}	210	200	30	2.0-4.5	Li-ion
Iron Fluoride@CMK-3 Nanocomposite[16]	23.7-2370 mAh g^{-1}	200	180	45	1.5-4.5	Li-ion

Iron Fluoride@CMK-3 Nanocomposite[16]	2.37- 11.85 Ah g^{-1}	110	105	145	1.5-4.5	Li-ion
$FeF_3*0.33H_2O$[17]	71 mAh g^{-1}	126	105	30	1.6-4.5	Li-ion
FeF_3 nanowires [18]	50 mAh g^{-1}	543	223	50	1.5-4.5	Li-ion
FeF_3 - graphene nanocomposites[19]	45 mAh g^{-1}	210	205	30	2.0-4.5	Li-ion
FeF_3 - graphene nanocomposites[19]	71.2 mAh g^{-1}	620	490	20	1.5-4.5	Li-ion
Macroporous FeF_3[20]	20 mAh g^{-1}	210	190	30	2.0-4.5	Li-ion
Graphene-wrapped FeF_3 nanocrystals[21]	20.8 mAh g^{-1}	280	185.6	100	1.5-4.5	Li-ion
FeF_3[22]	20 mAh g^{-1}	224	143	100	2.0-4.5	Li-ion
BiF_3 nanocrystals[23]	50 mAh g^{-1}	320	170	10	2.0-4.0	Li-ion
$FeF_3*0.33H_2O$/C nanocomposites[24]	119 mAh g^{-1}	160	140	100	2.0-4.5	Li-ion
FeF_3 nanocomposite[25]	10-80 mAh g^{-1}	200	175	55	2.0-4.5	Li-ion

References

(1) Wei, Z.; Filatov, A. S.; Dikarev, E. V. Volatile Heterometallic Precursors for the Low-Temperature Synthesis of Prospective Sodium Ion Battery Cathode Materials. *J. Am. Chem. Soc.* **2013,** *135*, 12216-12219.

(2) Toby, B. H.; Von Dreele, R. B. GSAS-II: the genesis of a modern open-source all purpose crystallography software package. *J. Appl. Crystallogr.* **2013,** *46*, 544-549.

(3) Benner, G.; Hoppe, R. Divalent iron fluorides. 1. The structure of NaFeF3. *J. Fluorine Chem.* **1990,** *46*, 283-295.

(4) Arai, H.; Okada, S.; Sakurai, Y.; Yamaki, J.-i. Cathode Performance and Voltage Estimation of Metal Trihalides. *J. Power Sources* **1997,** *68*, 716-719.

(5) Badway, F.; Cosandey, F.; Pereira, N.; Amatucci, G. G. Carbon Metal Fluoride Nanocomposites: High-Capacity Reversible Metal Fluoride Conversion Materials as Rechargeable Positive Electrodes for Li Batteries. *J. Electrochem. Soc.* **2003,** *150*, A1318-A1327.

(6) Kitajou, A.; Komatsu, H.; Chihara, K.; Gocheva, I. D.; Okada, S.; Yamaki, J.-i. Novel Synthesis and Electrochemical Properties of Perovskite-Type $NaFeF_3$ for a Sodium-Ion Battery. *J. Power Sources* **2012,** *198*, 389-392.

(7) Yamada, Y.; Doi, T.; Tanaka, I.; Okada, S.; Yamaki, J.-i. Liquid-phase Synthesis of Highly Dispersed $NaFeF_3$ Particles and Their Electrochemical Properties for Sodium-ion Batteries. *J. Power Sources* **2011,** *196*, 4837-4841.

(8) Gocheva, I. D.; Nishijima, M.; Doi, T.; Okada, S.; Yamaki, J.-i.; Nishida, T. Mechanochemical Synthesis of $NaMF_3$ (M = Fe, Mn, Ni) and Their Electrochemical Properties as Positive Electrode Materials for Sodium Batteries. *J. Power Sources* **2009,** *187*, 247-252.

(9) Sun, S.; Shi, Y.; Bian, S.; Zhuang, Q.; Liu, M.; Cui, Y. Enhanced charge storage of Na3FeF6 with carbon nanotubes for lithium-ion batteries. *Solid State Ionics* **2017,** *312*, 61-66.

(10) Nishijima, M.; Gocheva, I. D.; Okada, S.; Doi, T.; Yamaki, J.-i.; Nishida, T. Cathode Properties of Metal Trifluorides in Li and Na Secondary Batteries. *J. Power Sources* **2009,** *190*, 558-562.

(11) Dimov, N.; Nishimura, A.; Chihara, K.; Kitajou, A.; Gocheva, I. D.; Okada, S. Transition Metal $NaMF_3$ Compounds as Model Systems for Studying the Feasibility of Ternary Li-M-F and Na-M-F Single Phases as Cathodes for Lithium–Ion and Sodium–Ion Batteries. *Electrochimica Acta* **2013,** *110*, 214-220.

(12) Bai, Y.; Zhou, X.; Zhan, C.; Ma, L.; Yuan, Y.; Wu, C.; Chen, M.; Chen, G.; Ni, Q.; Wu, F., et al. 3D Hierarchical Nano-Flake/Micro-Flower Iron Fluoride with Hydration Water Induced Tunnels for Secondary Lithium Battery Cathodes. *Nano Energy* **2017,** *32*, 10-18.

(13) Di Carlo, L.; Conte, D. E.; Kemnitz, E.; Pinna, N. Microwave-Assisted Fluorolytic Sol-Gel Route to Iron Fluoride Nanoparticles for Li-Ion Batteries. *Chem. Commun.* **2014,** *50*, 460-462.

(14) Guntlin, C. P.; Zünd, T.; Kravchyk, K. V.; Wörle, M.; Bodnarchuk, M. I.; Kovalenko, M. V. Nanocrystalline FeF_3 and MF_2 (M = Fe, Co, and Mn) from Metal Trifluoroacetates and Their Li(Na)-Ion Storage Properties. *J. Mater. Chem. A* **2017,** *5*, 7383-7393.

(15) Kim, S. W.; Seo, D. H.; Gwon, H.; Kim, J.; Kang, K. Fabrication of FeF_3 Nanoflowers on CNT Branches and Their Application to High Power Lithium Rechargeable Batteries. *Adv. Mater.* **2010,** *22*, 5260-5264.

(16) Li, B.; Zhang, N.; Sun, K. Confined Iron Fluoride@CMK-3 Nanocomposite as an Ultrahigh Rate Capability Cathode for Li-Ion Batteries. *Small* **2014,** *10*, 2039-2046.

(17) Li, C.; Gu, L.; Tsukimoto, S.; van Aken, P. A.; Maier, J. Low-Temperature Ionic-Liquid-Based Synthesis of Nanostructured Iron-Based Fluoride Cathodes for Lithium Batteries. *Adv. Mater.* **2010,** *22*, 3650-3654.

(18) Li, L.; Meng, F.; Jin, S. High-capacity Lithium-ion Battery Conversion Cathodes Based on Iron Fluoride Nanowires and Insights Into the Conversion Mechanism. *Nano Lett.* **2012,** *12*, 6030-6037.

(19) Liu, J.; Wan, Y.; Liu, W.; Ma, Z.; Ji, S.; Wang, J.; Zhou, Y.; Hodgson, P.; Li, Y. Mild and Cost-Effective Synthesis of Iron Fluoride-Graphene Nanocomposites for High-Rate Li-Ion Battery Cathodes. *J. Mater. Chem. A* **2013,** *1*, 1969-1975.

(20) Ma, D. L.; Cao, Z. Y.; Wang, H. G.; Huang, X. L.; Wang, L. M.; Zhang, X. B. Three-Dimensionally Ordered Macroporous FeF_3 and its in situ Homogenous Polymerization Coating for High Energy and Power Density Lithium Ion Batteries. *Energy Environ. Sci.* **2012,** *5*, 8538-8542.

(21) Ma, R.; Lu, Z.; Wang, C.; Wang, H. E.; Yang, S.; Xi, L.; Chung, J. C. Large-Scale Fabrication of Graphene-Wrapped FeF_3 Nanocrystals as Cathode Materials for Lithium Ion Batteries. *Nanoscale* **2013,** *5*, 6338-6343.

(22) Myung, S. T.; Sakurada, S.; Yashiro, H.; Sun, Y. K. Iron Trifluoride Synthesized via Evaporation Method and Its Application to Rechargeable Lithium Batteries. *J. Power Sources* **2013,** *223*, 1-8.

(23) Oszajca, M. F.; Kravchyk, K. V.; Walter, M.; Krieg, F.; Bodnarchuk, M. I.; Kovalenko, M. V. Colloidal BiF_3 Nanocrystals: A Bottom-Up Approach to Conversion-Type Li-Ion Cathodes. *Nanoscale* **2015,** *7*, 16601-16605.

(24) Tan, J. L.; Liu, L.; Hu, H.; Yang, Z. H.; Guo, H. P.; Wei, Q. L.; Yi, X.; Yan, Z. C.; Zhou, Q.; Huang, Z. F., et al. Iron Fluoride with Excellent Cycle Performance Synthesized by Solvothermal Method as Cathodes for Lithium Ion Batteries. *J. Power Sources* **2014,** *251*, 75-84.

(25) Yabuuchi, N.; Sugano, M.; Yamakawa, Y.; Nakai, I.; Sakamoto, K.; Muramatsu, H.; Komaba, S. Effect of Heat-Treatment Process on FeF_3 Nanocomposite Electrodes for Rechargeable Li Batteries. *J. Mater. Chem.* **2011,** *21*, 10035-10041.